Surface & Coatings Technology xxx (xxxx) xxx–xxx

Contents lists available at ScienceDirect

Surface & Coatings Technology

journal homepage: www.elsevier.com/locate/surfcoat

Sample size effect on micro-mechanical properties of gold electroplated with dense carbon dioxide

Haochun Tang[a,b,*], Ken Hashigata[a,b], Tso-Fu Mark Chang[a,b], Chun-Yi Chen[a,b], Takashi Nagoshi[c], Daisuke Yamane[a,b], Toshifumi Konishi[a,b,d], Katsuyuki Machida[a,b], Kazuya Masu[a,b], Masato Sone[a,b]

[a] Institute of Innovative Research, Tokyo Institute of Technology, 4259 Nagatsuta-cho, Midori-ku, Yokohama 226-8503, Japan
[b] CREST, Japan Science and Technology Agency, 4259 Nagatsuta-cho, Midori-ku, Yokohama 226-8503, Japan
[c] National Institute of Advanced Industrial Science and Technology, 1-2-1 Namiki, Tsukuba, Ibaraki 305-8564, Japan
[d] NTT Advanced Technology Corporation, 3-1 Morinosato Wakamiya, Atsugi-shi, Kanagawa 243-0124, Japan

ARTICLE INFO

Keywords:
Electroplated gold
Dense carbon dioxide
Micro-compression
Size effect

ABSTRACT

Micro-mechanical properties of gold electroplated with dense carbon dioxide contained electrolyte (EP-DCE) were investigated by micro-compression tests using micro-pillar specimens for applications as movable components in MEMS devices. The effect of grain size on the micro-mechanical properties was also investigated using a gold film fabricated by conventional electroplating (CONV-EP). The gold film fabricated by the EP-DCE showed a finer average grain size when compared with that of the CONV-EP. Because of the finer grain size, the micro-pillar fabricated from the EP-DCE film showed a higher strength than that of the micro-pillar fabricated from the CONV-EP. An increase in the compressive flow stress from 740 to 810 MPa was observed as dimensions of the micro-pillars decreased from 20 × 20 × 40 to 10 × 10 × 20 μm^3, which was a result of the sample size effect.

1. Introduction

Gold materials prepared by electroplating (EP) are widely used in electronics industries as conducting materials for interconnections owing to their superior properties such as high chemical stability, corrosion resistance, electrical conductivity, and density [1,2]. Recently, micro-electronic-mechanical systems (MEMS) accelerometers utilizing movable components made of gold-based materials were reported to have better sensitivity than the conventional silicon-based devices [3]. However, gold is known to be a relatively soft material (i.e., yield strength of bulk gold: 55–200 MPa [4]), especially when compared with the silicon [5]. The low mechanical strength becomes a concern in further miniaturization of the device. Therefore, strengthening of the gold materials is required to allow further improvement of the MEMS accelerometer.

Grain boundary strengthening mechanism based on Hall–Petch relationship is often applied in strengthening of metallic materials [6–8]. Strengthening of the metallic materials is achieved when the average grain size (d_g) reaches submicron- or nano-scale [9]. On the other hand, d_g of electroplated metallic materials can be easily controlled by the electroplating parameters such as the current density, pH value, and plating bath temperature [10–12]. An alternative electroplating process conducted in high pressure environment, pressurized by introducing dense carbon dioxide into the electrolyte, was reported to be effective to refine the d_g to nano-scale (d_g < 100 nm) as demonstrated in electroplating of Ni and Cu [13–16]. A significant enhancement in the mechanical property was reported in Ni films fabricated by the electroplating with dense carbon dioxide contained electrolyte (EP-DCE) method [17]. Through application of the EP-DCE, further grain refinement in d_g of the electroplated gold can be realized and leads to further enhancement in the mechanical strength.

Mechanical properties of materials having dimensions in micro-scale are different from those of bulk materials. The phenomenon is known as the sample size effect. Since the first report of the sample size effect in single crystal specimens [18], many subsequent investigations have demonstrated the effect in the mechanical strength of specimens composed of fcc and bcc metals when dimensions of the specimen are decreased to micro- or nano-scale [19,20].

In order to utilize the grain boundary strengthening mechanism, the specimen evaluated in this study will be fabricated from gold films prepared by the EP-DCE method, which will be composited of gold crystals having the d_g in nano-scale order [21]. Components in MEMS devices often have dimensions in micrometer or tens of micrometer order. For practical applications of the EP-DCE in fabrication of

* Corresponding author.
E-mail address: tang.h.ab@m.titech.ac.jp (H. Tang).

https://doi.org/10.1016/j.surfcoat.2018.02.041
Received 15 November 2017; Received in revised form 19 January 2018; Accepted 12 February 2018

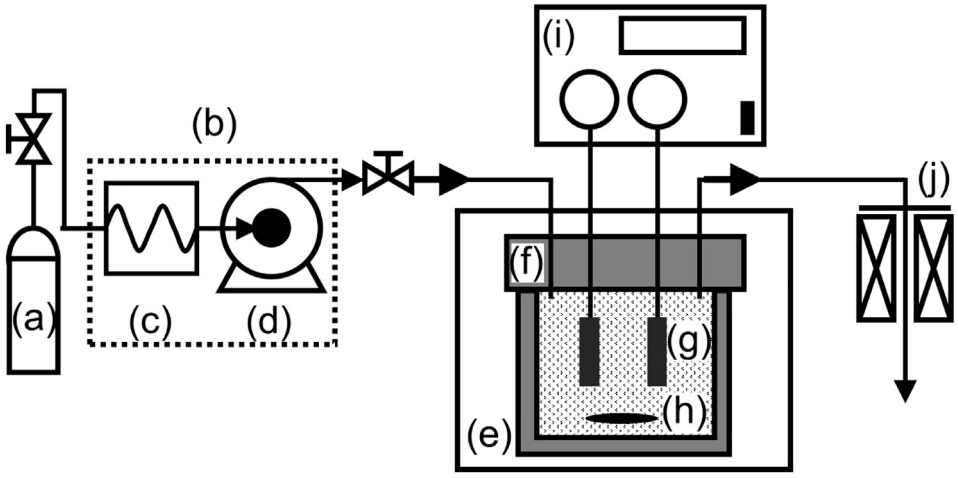

Fig. 1. High pressure apparatus: (a) CO_2 gas tank, (b) CO_2 pressurization unit, (c) liquidization unit, (d) high-pressure pump, (e) box oven, (f) reaction cell, with PEEK coating on the inner wall, (g) substrates, (h) stirrer, (i) programmable power supply, and (j) back-pressure regulator.

components used in MEMS devices, it is necessary to evaluate the mechanical property using specimens having dimensions in micro-scale. For polycrystalline specimens, there are limited reportes on the sample size effect [22–24], especially for specimens composed of gold and having dimensions in micro-scale.

In this study, mechanical properties of gold films fabricated by the EP-DCE will be investigated by micro-compression tests using non-tapered micro-pillars fabricated from the electroplated gold films. Gold micro-pillars with three different dimensions, which are 20 × 20 × 40, 15 × 15 × 30, and 10 × 10 × 20 μm^3, and the same aspect ratio would be fabricated by focus ion beam (FIB) system. Micro-compression tests with a displacement controlled mode would be applied to evaluate the mechanical property.

2. Experimental

Details of the high pressure electroplating apparatus are shown in Fig. 1. The gold electrolyte used in this study was a commercially available sulfite-based gold electrolyte purchased from Matex Japan (Matex Gold NCA). The electrolyte was composed of 50 g/L of Na_2SO_3, 50 of g/L $(NH_4)_2SO_3$, 21.63 g/L of $Na_3[Au(SO_3)_2]$ with pH of 8.0 and 5% sodium gluconate. For the EP-DCE, pressure in the reaction cell was elevated by pressuring liquefied CO_2 into the cell and was controlled at 10 MPa during the entire electroplating process by a back-pressure regulator. A piece of gold film fabricated by the conventional electroplating (CONV-EP) method, which was conducted at atmospheric pressure, was prepared to be used as a comparison with the EP-DCE. The current density and the plating temperature for both CONV-EP and EP-DCE were fixed at 5 mA/cm^2 and 40 °C, respectively. Cu plates and Pt plates with the same dimensions of 1.0 × 2.0 cm^2 were used as the cathode and the anode, respectively. Thickness of the gold films was controlled at about 50 μm.

Micro-pillars with a square cross-section and an aspect ratio of 2:1, which is the long-side over one side of the square cross-section, were fabricated from the gold films using FIB (Hitachi FIB-2100). Dimensions of the micro-pillars were either 20 × 20 × 40, 15 × 15 × 30, or 10 × 10 × 20 μm^3. Details of the fabrication method are reported in a previous work [17]. The Ga ion implantation from the FIB fabrication process is ignored due to shallow penetration depth of the Ga ions (less than few tens of nanometer) [25,26] when compared to dimensions of the specimen evaluated in this study. The micro-compression test was performed with a testing machine equipped with a diamond flat-punch indenter. The micro-compression test was conducted at a constant displacement rate of 0.1 μm/s using a piezo-electric actuator. A strain gage type load cell was used to record the data of displacement and load at a rate of 30 points per second. The engineering strain-stress (*SS*) curves were subsequently converted by the following equations:

$$\sigma = P/A_0 \quad (1)$$

$$\varepsilon = L/L_0 \quad (2)$$

where σ is the engineering stress, P is the load, A_0 is area of top surface of the micro-pillar, ε is the engineering strain, L is the displacement, L_0 is the length of micro-pillar. The microstructure and deformation behaviors of the gold micro-pillars were observed using a scanning ion microscope (SIM) equipped within the FIB and a scanning electron microscope (SEM, JEOL 7500F).

3. Results and discussion

3.1. Mechanical properties of gold micro-pillars with different grain size

Fig. 2 shows SIM images of the micro-pillars fabricated from the CONV-EP and the EP-DCE gold films before and after the micro-compression tests. Dimensions of the two pillars were both 20 × 20 × 40 μm^3. Camouflage-like patterns were observed on surface of side-wall of the CONV-EP pillar. Different level of brightness observed in the patterns of SIM image, as shown in Fig. 2(a) and (b), are usually results of the difference in crystal orientation. Hence, boundaries of the patterns are often identified as boundaries of grains. For the CONV-EP gold film, the d_g was ranged in several hundreds of nanometer as shown in the SIM image. d_g of the CONV-EP film prepared under the same condition was ~0.8 μm evaluated by electron backscatter diffraction reported in a previous study [21]. After the compression test, the pillar showed typical deformation behaviors of polycrystalline structures [23], which the pillar deformed into the shape of a barrel as shown in Fig. 2(b).

On the other hand, patterns with different level of brightness were also observed on surfaces of the EP-DCE pillar, but the sizes were much smaller than those in the CONV-EP pillar, which implied d_g of the EP-DCE film was much smaller than that of the CONV-EP film. The d_g was roughly estimated from side-wall of the EP-DCE pillar, Fig. 2(c), and the d_g was below 100 nm. In a previous study on gold electroplating with dense carbon dioxide, the gold film fabricated under the same conditions used in this study showed an average grain size at ~13 nm [21]. The grain refinement effect observed in the EP-DCE film is suggested to be caused by the same mechanisms reported in electroplating of Ni using the EP-DCE, which are the periodic-plating-characteristics (PPC) [14] and co-deposition of carbon contents from reduction of carbon dioxide dissociated in the electrolyte [13,16,21]. Similar barrel-shape deformation behavior was observed in the EP-DCE pillar after the

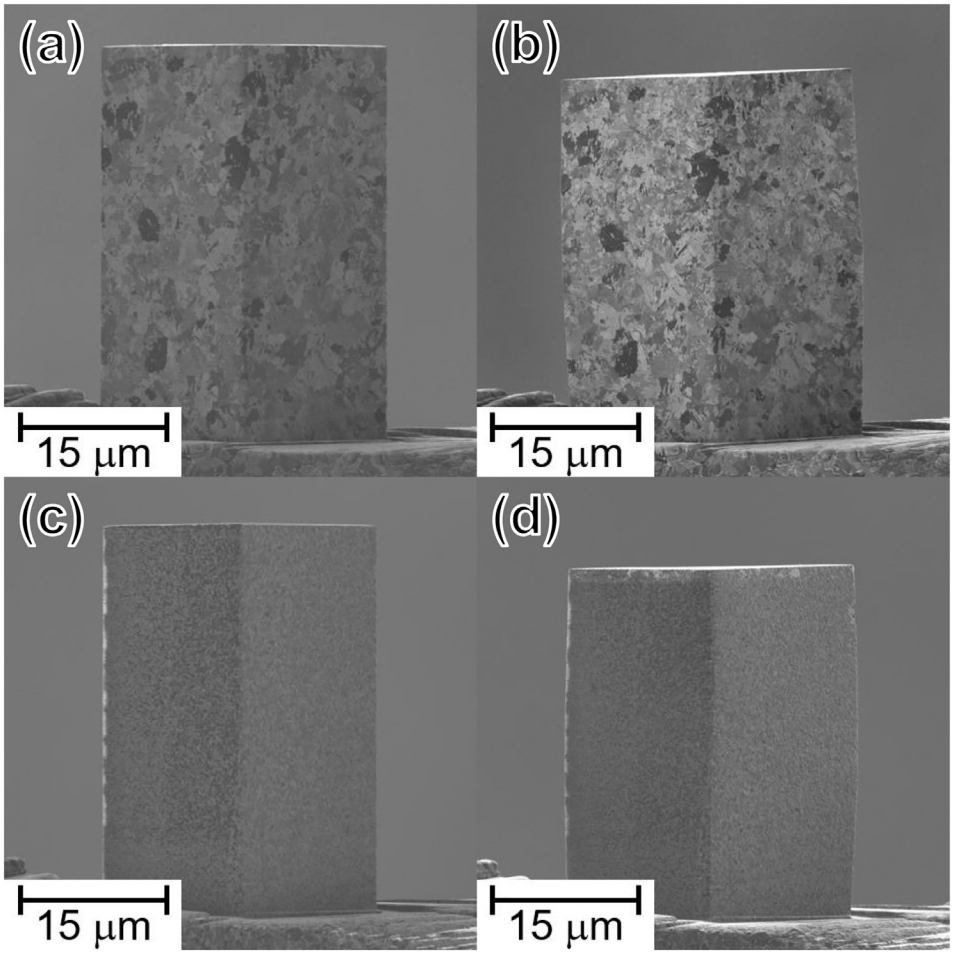

Fig. 2. SIM images of the CONV-EP pillar (a) before and (b) after the compression test and the EP-DCE micro-pillar (c) before and (d) after the micro-compression test. Dimensions of the two pillars were 20 × 20 × 40 μm^3.

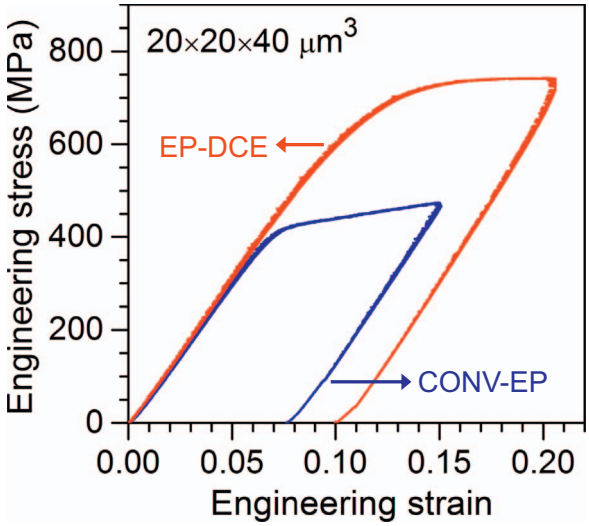

Fig. 3. Engineering *SS* curves of the gold micro-pillars fabricated from the CONV-EP and the EP-DCE gold films. (For interpretation of the references to color in this figure legend, the reader is referred to the web version of this article.)

compression test as shown in Fig. 2(d). Fig. 3 shows engineering strain-stress (*SS*) curves of the CONV-EP and the EP-DCE pillars obtained from the micro-compression tests. For *SS* curves generated from micro-mechanical tests, the yield point is usually unclear, and the 0.2% yield stress (σ_y) is determined, which is the cross-point of the *SS* curve and 0.2% strain offset line of the elastic deformation region. In addition to the σ_y, the flow stress (σ_f) was also determined, which is defined as the cross-point of the *SS* curve and 5% strain offset line of the elastic deformation region. The EP-DCE pillar showed the σ_y and the σ_f at 520 MPa and 740 MPa, respectively, which were both higher than those of the CONV-EP pillar. The σ_y and the σ_f of the CONV-EP pillar were 380 MPa and 460 MPa, respectively. The results confirmed that both of the gold micro-pillars exhibited higher mechanical strengths than those of the bulk-size gold [4,7,8], and the results were mostly because of synergistic effects of the sample size effect and the grain boundary strengthening mechanism. In addition, the EP-DCE gold film exhibited higher mechanical strengths than those of the CONV-EP pillar because of the finer d_g and the grain boundary strengthening mechanism. Strengths of polycrystalline materials are increased with a decrease in the d_g as explained by the Hall–Petch relationship [6].

3.2. Mechanical properties of the EP-DCE gold pillars with different dimension

Considering dimensions of the components in MEMS devices, mechanical properties of pillars having dimensions in 15 × 15 × 30 μm^3 and 10 × 10 × 20 μm^3 fabricated from the EP-DCE gold were also evaluated. The two micro-pillars were fabricated from the same EP-DCE gold film used in previous section. Therefore, the three pillars fabricated from the same gold film would have the same d_g. SEM images of the three EP-DCE pillars before and after the compression tests are shown in Fig. 4. After the compression tests, shown in Fig. 4(b), (d), and (f), the three pillars all showed the same barrel-shape deformation

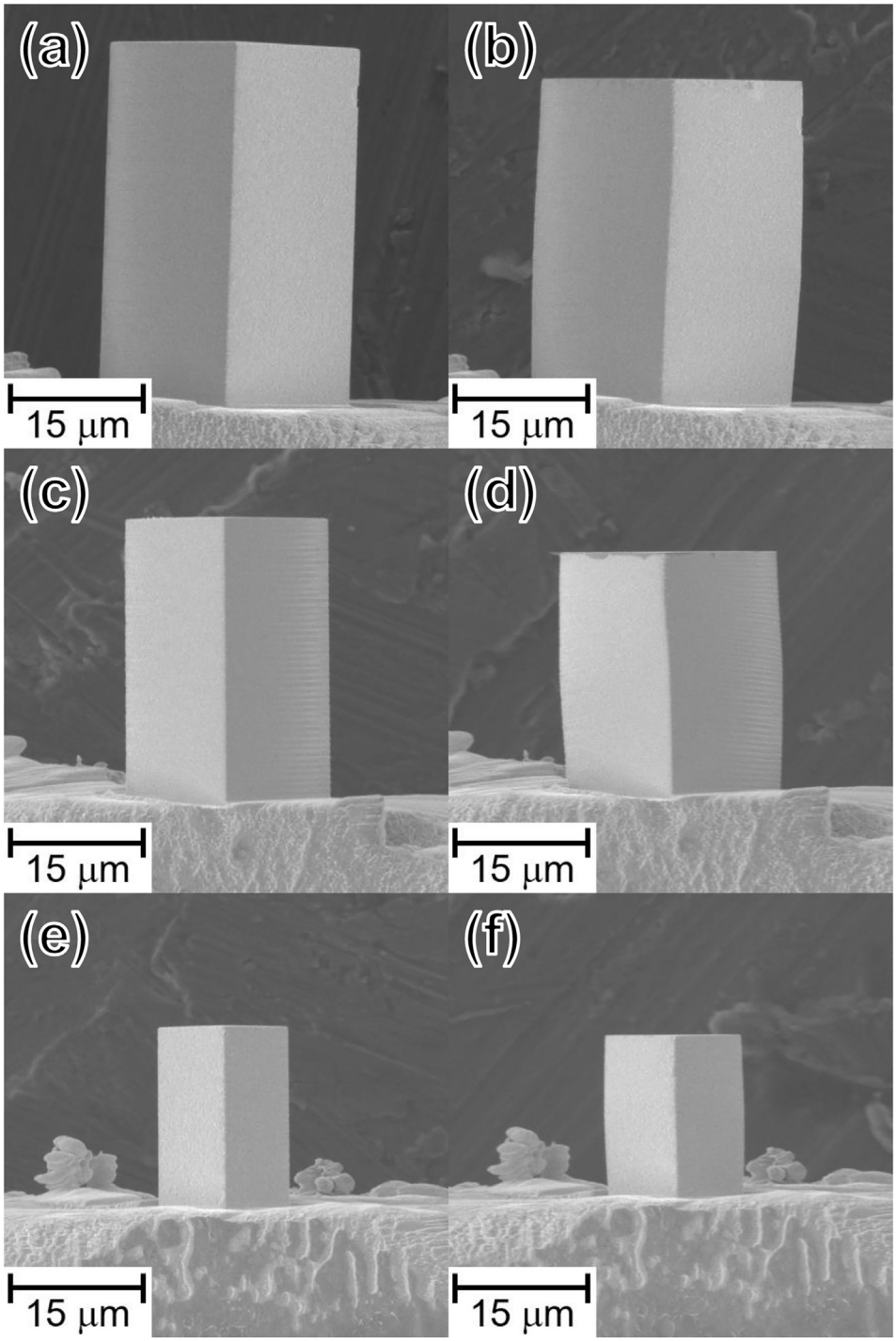

Fig. 4. SEM images of the EP-DCE micro-pillars (a, c, e) before and (b, d, f) after the micro-compression tests. Pillar dimensions: (a, b) 20 × 20 × 40 μm^3; (c, d) 15 × 15 × 30 μm^3; (e, f) 10 × 10 × 20 μm^3.

behavior.

Fig. 5 shows *SS* curves of the EP-DCE pillars with dimensions ranged from 10 × 10 × 20 to 20 × 20 × 40 μm^3. An increase in the σ_f in the plastic deformation region with a decrease in the sample size was observed. In a study on micro-pillars composed of nanocrystalline Ni having the d_g at 8 nm, an increase in the σ_f is reported when the pillar's cross-sectional area is decreased from 900 to 25 μm^2 [22]. The dependency of mechanical properties on the diameter or cross-sectional area of the samples evaluated is known as the sample size effect. In this study, the micro-pillars evaluated were also composed of metallic crystals having the d_g in nano-scale, and an enhancement in the strength was observed when the cross-section area decreased from 400 to 100 μm^2, which indicated the sample size effect in the EP-DCE pillars. The stress as a function in log scale of the pillar size (l, length of a side of the square cross-section) for the EP-DCE gold was plotted to further clarify the sample size effect. Rinaldi et al. [27] reported that compressive stresses of Ni pillars composed of nanocrystals exhibit an inverse power-law relationship with the diameter (D), $\sigma \propto D^{-\beta}$, where the value of β ranges from 0.38 to 0.66. Similar trends between the stresses with square root of the cross-sectional area, which is diameter of a pillar having circular cross-section or length of one side of a pillar having square cross-section as in this study, are reported in other

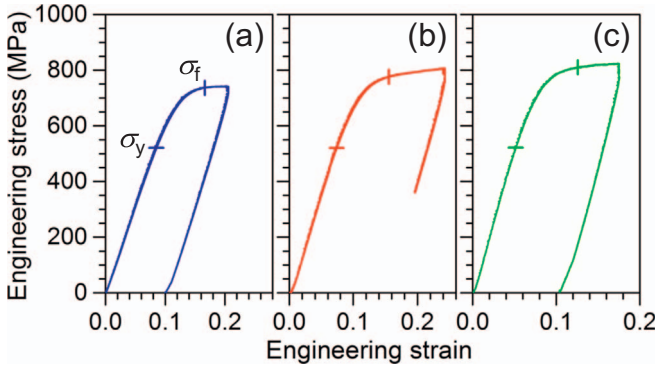

Fig. 5. Engineering *SS* curves of the EP-DCE pillars with different pillar sizes. (a) $20 \times 20 \times 40\,\mu m^3$, (b) $15 \times 15 \times 30\,\mu m^3$, and (c) $10 \times 10 \times 20\,\mu m^3$. The yield strength ($\sigma_y$) and flow stress at 5% (σ_f) are marked by the vertical bar and horizontal bar, respectively.

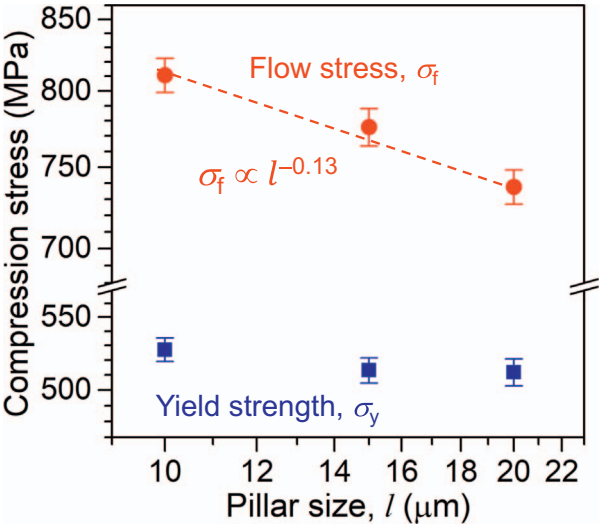

Fig. 6. Plot of the stress, σ_f and σ_y, versus the pillar size, l.

literature [22,28]. As shown in Fig. 6, the σ_f increased from 740 to 810 MPa when the l scales down from 20 to 10 μm, and the exponent is about −0.13, which gives $\sigma_f \propto l^{-0.13}$.

Mechanical properties determined from *SS* curves can be affected by the strain rate as reported in the literature, especially for nanocrystalline face-centered cubic metals, which the strength is reported to have an inverse power-law relationship with the strain rate, $\sigma \propto (strain\ rate)^{-m}$, and the m value is the strain rate sensitivity ranges from 0.01 to 0.03 [29–32]. In this study, the compression tests conducted were displacement rate controlled at 0.1 μm/s. Heights of the pillars evaluated were ranged from 40 to 20 μm, and the strain rate would be varied from 2.5×10^{-3} to $5.0 \times 10^{-3}\,s^{-1}$. Using the m value at 0.03, ~2.1% increase in the strength is expected when the strain rate is increased from 2.5×10^{-3} to $5.0 \times 10^{-3}\,s^{-1}$. In this study, the σ_f increased from 740 to 810 MPa when the strain rate was increased from 2.5×10^{-3} to $5.0 \times 10^{-3}\,s^{-1}$, which is ~9.5% increase in the strength. Therefore, the increase in the σ_f is suggested to be mainly contributed by the sample size effect.

On the other hand, there was almost no variation in the σ_y as the l changed, which remained at 520 MPa. For the sample size effect on the σ_y, ratio of the l to the d_g is important. The sample size effect on the σ_y is suggested to be observable when the l/d_g ratio is between 5–10 [23,32,33]. In this study, d_g of the EP-DCE gold film was finer than 100 nm and would lead to a ratio of $l/d_g \geq 100$ when the l was larger than 10 μm. This should be the main reason why the sample size effect showed insignificant influence on the σ_y.

4. Conclusions

Micro-mechanical properties of pillars having dimensions varied from $20 \times 20 \times 40$ to $10 \times 10 \times 20\,\mu m^3$ fabricated from a piece of gold film electroplated with dense carbon dioxide contained electrolyte were evaluated by micro-compression tests for applications as micro-components in MEMS devices. The EP-DCE gold micro-pillars were composed of grains having an average size less than 100 nm. A pillar with dimensions of $20 \times 20 \times 40\,\mu m^3$ fabricated from a gold film with a larger d_g at ~0.8 μm was also evaluated to be used as a comparison with the EP-DCE pillar. The EP-DCE pillar showed a higher strength than the pillar composed of a larger d_g because of the grain boundary strengthening mechanism. For the EP-DCE pillars with different pillar dimensions, the σ_f increased from 740 to 810 MPa with a decrease in the pillar dimensions from $20 \times 20 \times 40$ to $10 \times 10 \times 20\,\mu m^3$. The strengthening observation confirmed the sample size effect on mechanical properties of micro-pillars composed of gold crystals having an average grain size in the nano-scale. The results obtained in this study are valuable to be used in design of gold-based micro-components in MEMS devices.

Acknowledgement

This work is supported by the CREST Project (#14531864) operated by the Japan Science and Technology Agency (JST).

References

[1] M. Kato, Y. Okinaka, Some recent developments in non-cyanide gold plating for electronics applications, Gold Bull. 37 (2004) 37–44.
[2] T.A. Green, Gold electrodeposition for microelectronic, optoelectronic and micro-system applications, Gold Bull. 40 (2007) 105–114.
[3] D. Yamane, T. Konishi, T. Matsushima, K. Machida, H. Toshiyoshi, K. Masu, Design of sub-1g microelectromechanical systems accelerometers, Appl. Phys. Lett. 104 (2014) 074102.
[4] H. Espinosa, Plasticity size effects in free-standing submicron polycrystalline FCC films subjected to pure tension, J. Mech. Phys. Solids 52 (2004) 667–689.
[5] T. Tsuchiya, O. Tabata, J. Sakata, Y. Taga, Specimen size effect on tensile strength of surface-micromachined polycrystalline silicon thin films, J. Microelectromech. Syst. 7 (1998) 106–113.
[6] N.J. Petch, The cleavage strength of polycrystals, J. Iron Steel Inst. 174 (1953) 25–28.
[7] A. Leitner, V. Maier-Kiener, J. Jeong, M.D. Abad, P. Hosemann, S.H. Oh, D. Kiener, Interface dominated mechanical properties of ultra-fine grained and nanoporous Au at elevated temperatures, Acta Mater. 121 (2016) 104–116.
[8] V. Maier, A. Leitner, R. Pippan, D. Kiener, Thermally activated deformation behavior of ufg-Au: environmental issues during long-term and high-temperature nanoindentation testing, JOM 67 (2015) 2934–2944.
[9] D. Jia, K.T. Ramesh, E. Ma, Effects of nanocrystalline and ultrafine grain sizes on constitutive behavior and shear bands in iron, Acta Mater. 51 (2003) 3495–3509.
[10] A.M. Rashidi, A. Amadeh, The effect of saccharin addition and bath temperature on the grain size of nanocrystalline nickel coatings, Surf. Coat. Technol. 204 (2009) 353–358.
[11] T.-F.M. Chang, M. Sone, A. Shibata, C. Ishiyama, Y. Higo, Bright nickel film deposited by supercritical carbon dioxide emulsion using additive-free watts bath, Electrochim. Acta 55 (2010) 6469–6475.
[12] C.-Y. Chen, M. Yoshiba, T. Nagoshi, T.-F.M. Chang, D. Yamane, K. Machida, K. Masu, M. Sone, Pulse electroplating of ultra-fine grained au films with high compressive strength, Electrochem. Commun. 67 (2016) 51–54.
[13] S.-T. Chung, W.-T. Tsai, Effect of pressure on the electrodeposition of nanocrystalline Ni–C in supercritical CO_2 fluid, Thin Solid Films 518 (2010) 7236–7239.
[14] Y.-C. Chuang, S.-T. Chung, S.-Y. Chiu, C.-Y. Li, W.-T. Tsai, Effect of surfactant on the electrodeposition of Ni–P coating in emulsified supercritical CO_2 baths, Thin Solid Films 529 (2013) 322–326.
[15] T.-F.M. Chang, M. Sone, Function and mechanism of supercritical carbon dioxide emulsified electrolyte in nickel electroplating reaction, Surf. Coat. Technol. 205 (2011) 3890–3899.
[16] T.-F.M. Chang, T. Shimizu, C. Ishiyama, M. Sone, Effects of pressure on electroplating of copper using supercritical carbon dioxide emulsified electrolyte, Thin Solid Films 529 (2013) 25–28.
[17] T. Nagoshi, T.-F.M. Chang, S. Tatsuo, M. Sone, Mechanical properties of nickel fabricated by electroplating with supercritical CO_2 emulsion evaluated by micro-compression test using non-tapered micro-sized pillar, Microelectron. Eng. 110 (2013) 270–273.
[18] M.D. Uchic, D.M. Dimiduk, J.N. Florando, W.D. Nix, Sample dimensions influence strength and crystal plasticity, Science 305 (2004) 986–989.
[19] J.R. Greer, W.C. Oliver, W.D. Nix, Size dependence of mechanical properties of gold

at the micron scale in the absence of strain gradients, Acta Mater. 53 (2005) 1821–1830.
[20] M.D. Uchic, P.A. Shade, D.M. Dimiduk, Plasticity of micrometer-scale single crystals in compression, Annu. Rev. Mater. Res. 39 (2009) 361–386.
[21] H. Tang, C.-Y. Chen, T. Nagoshi, T.-F.M. Chang, D. Yamane, K. Machida, K. Masu, M. Sone, Enhancement of mechanical strength in au films electroplated with supercritical carbon dioxide, Electrochem. Commun. 72 (2016) 126–130.
[22] T. Nagoshi, M. Mutoh, T.-F.M. Chang, T. Sato, M. Sone, Sample size effect of electrodeposited nickel with sub-10 nm grain size, Mater. Lett. 117 (2014) 256–259.
[23] M. Dietiker, S. Buzzi, G. Pigozzi, J.F. Löffler, R. Spolenak, Deformation behavior of gold nano-pillars prepared by nanoimprinting and focused ion-beam milling, Acta Mater. 59 (2011) 2180–2192.
[24] R. Gu, A.H.W. Ngan, Size effect on the deformation behavior of duralumin micropillars, Scr. Mater. 68 (2013) 861–864.
[25] F. Machalett, K. Edinger, J. Melngailis, M. Diegel, K. Steenbeck, E. Steinbeiss, Direct patterning of gold oxide thin films by focused ion-beam irradiation, Appl. Phys. A Mater. Sci. Process. 71 (2000) 331–335.
[26] D. Kiener, C. Motz, M. Rester, M. Jenko, G. Dehm, FIB damage of Cu and possible consequences for miniaturized mechanical tests, Mater. Sci. Eng. A 459 (2007) 262–272.
[27] A. Rinaldi, P. Peralta, C. Friesen, K. Sieradzki, Sample-size effects in the yield behavior of nanocrystalline nickel, Acta Mater. 56 (2008) 511–517.
[28] R. Fritz, V. Maier-Kiener, D. Lutz, D. Kiener, Interplay between sample size and grain size: single crystalline vs. ultrafine-grained chromium micropillars, Mater. Sci. Eng. A 674 (2016) 626–633.
[29] N. Warthi, P. Ghosh, A.H. Chokshi, Approaching theoretical strengths by synergistic internal and external size refinement, Scr. Mater. 68 (2013) 225–228.
[30] R. Schwaiger, B. Moser, M. Dao, N. Chollacoop, S. Suresh, Some critical experiments on the strain-rate sensitivity of nanocrystalline nickel, Acta Mater. 51 (2003) 5159–5172.
[31] Q. Wei, Strain rate effects in the ultrafine grain and nanocrystalline regimes—influence on some constitutive responses, J. Mater. Sci. 42 (2007) 1709–1727.
[32] J.Y. Zhang, G. Liu, J. Sun, Strain rate effects on the mechanical response in multi- and single-crystalline Cu micropillars: grain boundary effects, Int. J. Plast. 50 (2013) 1–17.
[33] C. Howard, D. Frazer, A. Lupinacci, S. Parker, R.Z. Valiev, C. Shin, B.W. Choi, P. Hosemann, Investigation of specimen size effects by in-situ microcompression of equal channel angular pressed copper, Mater. Sci. Eng. A 649 (2016) 104–113.